Potentiation of paclitaxel activity by the HSP90 inhibitor 17-allylamino-17-demethoxygeldanamycin in human ovarian carcinoma cell lines with high levels of activated AKT

Nivedita Sain,[1] Bhavani Krishnan,[1] Michael G. Ormerod,[1] Assunta De Rienzo,[1] Wai M. Liu,[1] Stanley B. Kaye,[1] Paul Workman,[2] and Ann L. Jackman[1]

[1]Section of Medicine and [2]Cancer Research UK Centre for Cancer Therapeutics, The Institute of Cancer Research, Haddow Laboratories, Sutton, Surrey, United Kingdom

Abstract

Activation of the phosphatidylinositol-3-kinase (PI3K)/AKT survival pathway is a mechanism of cytotoxic drug resistance in ovarian cancer, and inhibitors of this pathway can sensitize to cytotoxic drugs. The HSP90 inhibitor 17-allylamino-17-demethoxygeldanamycin (17-AAG) depletes some proteins involved in PI3K/AKT signaling, e.g., ERBB2, epidermal growth factor receptor (EGFR), and phosphorylated AKT (p-AKT). 17-AAG and paclitaxel were combined (at a fixed 1:1 ratio of their IC_{50}) in four ovarian cancer cell lines that differ in expression of p-AKT, EGFR, and ERBB2. The EGFR-overexpressing A431 and KB epidermoid cell lines were also included. Combination indices (CI) were calculated using the median-effect equation and interpreted in the context of 17-AAG-mediated inhibition of PI3K signaling. Synergy was observed in IGROV-1- and ERBB2-overexpressing SKOV-3 ovarian cancer cells that express a high level of constitutively activated p-AKT [CI at fraction unaffected $(fu)_{0.5}$ = 0.50 and 0.53, respectively]. Slight synergy was observed in A431 cells (moderate p-AKT/overexpressed EGFR; CI at $fu_{0.5}$ = 0.76) and antagonism in CH1 (moderate p-AKT), HX62 cells (low p-AKT), and KB cells (low p-AKT/overexpressed EGFR; CI at fu_{50} = 3.0, 3.5, and 2.0, respectively). The observed effects correlated with changes in the rate of apoptosis induction. 17-AAG induced a decrease in HSP90 client proteins (e.g., C-RAF, ERBB2, and p-AKT) or in downstream markers of their activity (e.g., phosphorylated extracellular signal-regulated kinase or p-AKT) in SKOV-3, IGROV-1, and CH1 cells at IC_{50} concentrations. A non–growth-inhibitory concentration (6 nmol/L) reduced the phosphorylation of AKT (but not extracellular signal-regulated kinase) and sensitized SKOV-3 cells to paclitaxel. In conclusion, 17-AAG may sensitize a subset of ovarian cancer to paclitaxel, particularly those tumors in which resistance is driven by ERBB2 and/or p-AKT. [Mol Cancer Ther 2006;5(5):1197–208]

Introduction

Novel agents that specifically inhibit molecular targets driving oncogenesis are proving to be exciting drugs for the treatment of cancer (1). However, in the first-line, single-agent setting, imatinib is the only small molecule that has thus far received regulatory approval for chronic myeloid leukemia and gastrointestinal stromal tumors (2). These tumors are largely driven by single molecular abnormalities, the BCR-ABL translocation, and constitutively activated mutated c-KIT, respectively. The more common solid tumors possess multiple abnormalities (3) and molecularly targeted agents may, therefore, (*a*) need to be used in selected subpopulations of patients or (*b*) need to inhibit multiple molecular targets. The monoclonal antibody trastuzumab is the only agent in which patient selection, based on amplification of ERBB2, has guided its usage (4). Preliminary data showing increased copy number of the *epidermal growth factor receptor* (*EGFR*) gene in responding colorectal cancer patients (5) may lead to selection of patients who will benefit from cetuximab, and the association of activating EGFR mutations in the kinase domain with efficacy of gefitinib or erlotinib in non–small cell lung cancer is also suggesting a way forward (6).

Clinical trials with monoclonal antibodies (targeting ERBB2, EGFR, and vascular endothelial growth factor) have indicated that the major effect on survival comes from combination schedules with chemotherapy (7). In contrast, large-scale randomized trials with small-molecule signaling inhibitors have mostly been negative and this has led to a more cautious approach to the development of combination therapy (7). This underscores the need to improve the predictive value of preclinical models by, for example, determining the molecular context for mechanisms of synergy and antagonism, and also emphasizes the importance of examining the effect of

Received 10/26/05; revised 2/17/06; accepted 3/7/06.

Grant support: Cancer Research UK program grant [CUK] C309/A2187 and Cancer Research UK Life Fellowship (P. Workman), [CUK] A2661 (A. De Rienzo and B. Krishnan), and [CUK] A2647 (S.B. Kaye).

The costs of publication of this article were defrayed in part by the payment of page charges. This article must therefore be hereby marked advertisement in accordance with 18 U.S.C. Section 1734 solely to indicate this fact.

Requests for reprints: Ann Jackman, The Haddow Laboratories, The Institute of Cancer Research, 15 Cotswold Road, Sutton, Surrey SM2 5NG, United Kingdom. Phone: 44-208-722-4284; Fax: 44-208-661-3541. E-mail: ann.jackman@icr.ac.uk

doi:10.1158/1535-7163.MCT-05-0445

factors such as scheduling and dose. In this way, it may be possible to select patients likely to benefit from combination chemotherapy and to suggest schedules most likely to succeed.

17-Allylamino-17-demethoxygeldanamycin (17-AAG) inhibits HSP90, a molecular chaperone that is important for the posttranslational folding and stability of several client proteins, a number of which are components of signal transduction pathways that are considered important targets for cancer therapy (8–12). Key client proteins include those important to signaling through the RAS/RAF/MEK/extracellular signal-regulated kinase (ERK) and phosphahtidylinositol-3-kinase (PI3K)/AKT pathways e.g., ERBB2, EGFR, C-RAF, and AKT (13). 17-AAG, by virtue of its effects on multiple proteins, may therefore overcome resistance to agents that have more specific pathway effects (8). Indeed, clinical studies with 17-AAG have shown its potential as a single agent (9, 14, 15). However, there may be additional potential for its use in combination with conventional agents because some of the pathways inhibited by 17-AAG are also implicated in cytotoxic drug resistance, e.g., the PI3K/AKT survival pathway (16). The outcome of such combinations may be increased therapeutic benefit as a result of either their independent (additive) drug action or as a result of their synergistic interaction.

Combination studies of 17-AAG and cytotoxic agents in breast, BCR-ABL-positive leukemia, and non–small cell lung cancer have shown the potential for synergy in some tumor cell lines (17–19). For example, Munster et al. (17) studied the combination of 17-AAG with paclitaxel in four breast cancer cell lines with different levels of ERBB2 expression. Synergistic growth inhibition was observed in the two high ERBB2-expressing cell lines, BT-474 and SKBr-3, and this effect was associated with an earlier onset of apoptosis. In the other breast cell lines, sensitization at the level of apoptosis was observed irrespective of ERBB2 expression levels. Studies have shown that 17-AAG-mediated inhibition of PI3K/AKT signaling is an important component of its cytotoxic sensitizing property (20, 21). This pathway is oncogenic in many tumor types, driving processes such as cell growth and proliferation, and of particular relevance to cytotoxic drug therapy, generating strong antiapoptotic survival signals (22, 23). 17-AAG can inhibit AKT activity via at least two mechanisms: (*a*) depletion of ERBB2 or other ERBB family members and (*b*) preventing HSP90-dependent conformational stability of phosphorylated AKT (p-AKT; refs. 10, 13). Studies in mice showed that doses of 17-AAG that had no single-agent activity were sufficient to lead to a reduction of ERBB2 protein and p-AKT protein levels and to sensitization of BT-474 xenografts to paclitaxel (21).

The PI3K/Akt pathway is frequently highly activated in ovarian cancer, most commonly through mutational activation of *PI3KCA* or overexpression of AKT2 (24, 25). Overall, at least 40% of ovarian tumors possess an activated AKT2 (26). Altomare et al. (24) reported that 68% of ovarian carcinomas displayed elevated p-AKT using immunostaining of tissue microarrays. There was a close association between positive staining for p-AKT and positive staining for the phosphorylated forms of downstream substrates, mTOR and GSK3β. Inhibition of PI3K with LY294002 increased cisplatin- or paclitaxel-induced apoptosis in some human ovarian tumor cell lines (24, 27, 28). Taxanes and platinum-based drugs are part of standard chemotherapy for patients with ovarian cancer. In view of (*a*) the importance of the PI3K/AKT pathway in ovarian cancer, (*b*) the ability of 17-AAG to inhibit this pathway as well as other important oncogenic pathways, and (*c*) the ability of 17-AAG to potentiate the effect of paclitaxel in breast cancer models, we were interested in investigating whether 17-AAG could sensitize human ovarian tumor cell lines to these drugs either through effects on PI3K/AKT signaling and/or via other HSP90-dependent signaling pathways.

Four human ovarian tumor cell lines, SKOV-3, IGROV-1, CH1, and HX62, were chosen from a molecularly characterized panel of eight ovarian tumor cell lines because they displayed a range of molecular abnormalities leading to different levels of p-AKT (Ser^{473}). We confirmed that SKOV-3 (overexpresses ERBB2) and IGROV-1 cells have a constitutively activated AKT (p-AKT) and also showed that CH1 and HX62 cells express lower p-AKT levels that are inducible and noninducible by serum, respectively. Continuous exposure of these cell lines to 17-AAG and paclitaxel led to synergistic growth inhibition in SKOV-3 and IGROV-1 cells but antagonistic activity in CH1 and HX62 cells. It was also possible to use very low or non–growth-inhibitory concentrations of 17-AAG to sensitize SKOV-3 and IGROV-1 cells to paclitaxel. A431 and KB epidermoid cell lines were included in some experiments as control lines with EGFR overexpression. Molecular studies are described that implicate the effect of 17-AAG on client proteins important for sustained PI3K/AKT signaling and evasion of apoptosis when challenged with paclitaxel in the observed synergy/sensitization outcomes.

Materials and Methods

Cell Culture and Reagents

CH1, HX62, PXN94 (Institute of Cancer Research, Surrey, United Kingdom; ref. 29), A2780 (30), and IGROV-1 (American Type Culture Collection, Manassas, VA) ovarian tumor cell lines and A431 and KB epidermoid tumor cell lines were cultured in DMEM without glutamine supplemented with 1% (v/v) nonessential amino acids, 2 mmol/L glutamine (Life Technologies, Ltd., Paisley, United Kingdom), and 10% heat-inactivated fetal bovine serum (PAA Laboratories, Somerset, United Kingdom; Invitrogen, Paisley, United Kingdom). SKOV-3 and OVCAR-4 ovarian tumor lines (American Type Tissue Collection) were cultured in RPMI medium without glutamine (Sigma-Aldrich, Gillingham, Dorset, United Kingdom) supplemented as described above. Cells were maintained in an incubator with a humidified atmosphere containing 5% CO_2 at 37°C.

17-AAG (kindly supplied by Dr. E. Sausville, National Cancer Institute, Washington, DC) and paclitaxel (Sigma-Aldrich, Poole, Dorset, United Kingdom) were dissolved in DMSO and ethanol, respectively, to give a stock solution of 10 mmol/L. A 20 mmol/L stock solution of carboplatin (Sigma-Aldrich) was made by dissolving in PBS. The stock solutions were stored for up to 3 months (17-AAG and carboplatin stored at −20°C and paclitaxel at 4°C). On the day of experiments, drug dilutions were made fresh by first diluting with unsupplemented medium to 0.2 mmol/L, thereby diluting the solvent concentration to 1%. Further drug dilutions were made in unsupplemented medium containing 1% solvent.

The following antibodies were used for immunoblotting: mouse monoclonal secondary antibodies (Amersham Biosciences, Buckinghamshire, United Kingdom) against C-RAF, HSP70 (Santa Cruz Biotechnology, Santa Cruz, CA), and glyceraldehyde-3-phosphate dehydrogenase (GAPDH; Chemicon Europe, Ltd., Hampshire, United Kingdom); rabbit polyclonal secondary antibodies (Amersham Biosciences) against ERBB2 (Upstate, NY), p-ERK, ERK, cyclin D1, p-AKT (Ser^{473}), AKT, p-mTOR, mTOR, p-GSK3β (Ser^{9}), GSK3β, and cleaved poly(ADP)ribose polymerase (PARP, Asp^{214}; New England Biolabs, Ltd., Hertfordshire, United Kingdom).

Combination Studies

Inhibition of Cell Growth. Exponentially growing CH1, SKOV-3, IGROV-1, HX62, A431, and KB tumor cells were harvested and plated (2,000 per well in a volume of 0.16 mL) in 96-well plates (Corning, c/o Sigma-Aldrich, Gillingham, Dorset, United Kingdom) and incubated at 37°C, 5% CO_2 for ~30 hours. A range of drug concentrations (prepared as described above) was then added (20 μL) to the wells either alone (plus 20 μL of solvent used for second drug used in the combination) or in combination (quadruplicate wells), giving a final volume of 200 μL/well. Control wells contained 20 μL of each relevant solvent (final concentration of each solvent was 0.1%). Incubation was for 72 hours (HX62, IGROV-1, A431, and KB) or 96 hours (SKOV-3 and CH1) sufficient to give approximately three to four population doublings. Cell growth was determined using an 3-(4,5-dimethylthiazol-2-yl)-2,5-diphenyltetrazolium bromide (MTT) assay as described previously (31).

Analysis. Most experiments were done combining both agents added together at a fixed ratio of the IC_{50} of each individual drug. The effects of the combination were calculated for each experimental condition using an in-house spreadsheet based on the median-effect analysis method of Chou and Talalay (32). For each level of fraction unaffected (fu), a combination index (CI) was calculated according to the following equation: $CI = (D)_1 / (D_f)_1 + (D)_2 / (D_f)_2 + [(D)_1 (D_f)_2 / (D_f)_1 (D_f)_2]$, where $(D)_1$ and $(D)_2$ are the concentrations of the combination required to produce a fu, and $(D_f)_1$ and $(D_f)_2$ are the concentrations of the individual drugs required to produce fu. Linear regression coefficients (r^2) of median-effect plots were required to be >0.95 for the data to qualify for analysis. A histogram is obtained in which CI values are given at various fu values. Only values obtained on the near linear part of the fu/dose plot are valid (generally between $fu_{0.2}$ and $fu_{0.8}$ depending on shape of curve). These data can also be used to generate a best-fit CI at $fu_{0.25}$, $fu_{0.50}$, and $fu_{0.75}$ (combined drug doses in a ratio of their IC_{50} that inhibit growth by 75%, 50%, and 25%, respectively). Occasionally, we rejected the CI at $fu_{0.25}$ or $fu_{0.75}$ when the actual data points at these fu values diverged from the fitted line. CI <1, CI ~1, and CI >1 indicates synergy, additivity, and antagonism, respectively. A one-sample *t* test (two-tailed) was used to compare the CI at $fu_{0.50}$ with 1 (GraphPad Prism 4.00 software; GraphPad Software, Inc., San Diego, CA). The data are also presented as the average CI of mean $fu_{0.25}$, $fu_{0.5}$, and $fu_{0.75}$.

Further studies were done in some cell lines in which the dose-response curve of paclitaxel was determined in the presence of a fixed, low concentration of 17-AAG (at a concentration that gave a fu ≥0.90). The fu values and CI were then calculated and analyzed using the equation of Chou and Talalay as described above.

Cell Number Measurements

Exponentially growing cells (5×10^4) were added to T25 flasks (Nunc A/S, Kamstrupvej, Denmark) in 4 mL medium. Approximately 30 hours later, drugs and/or solvent were added (total of 1 mL). Attached and detached cells were collected at 24, 48, and 72 hours and counted using a hemocytometer (Fisher Scientific, Loughborough, United Kingdom). Nuclei of detached cells were visually confirmed as being largely apoptotic after Geisma staining.

Immunoblotting

Adherent cells were grown to 30% to 50% confluence and then exposed to different agents, at various times and doses, as described in Results. After exposure, cells were harvested, washed with ice-cold PBS, resuspended in 150 μL cold lysis buffer [50 mmol/L Tris/150 mmol/L sodium chloride (pH 7.5), 1% IGEPAL CA-630, 0.1% SDS, 100 μg/mL phenylmethylsufonylfluoride, 10 μg/mL aprotinin, 20 μg/mL leupeptin, and 100 μmol/L sodium orthovanadate], left on ice for 15 minutes, and then centrifuged at 15,000 × *g* for 15 minutes at 4°C; the supernatant was stored at −70°C until required. Protein concentration for each lysate was determined using the BCA protein assay method (Sigma-Aldrich). Following solubilization of 80 to 100 μg protein in Laemmli buffer and boiling for 1 minute, the proteins were separated on precast 4% to 20% gradient Tris-glycine gels (Novex, Invitrogen, Paisley, United Kingdom) and transferred onto 0.45 μm nitrocellulose membranes (Invitrogen). These membranes were then probed with individual antibodies, using horseradish peroxidase–conjugated secondary antibodies, and visualized using the enhanced chemiluminescence plus detection system (Amersham Biosciences).

Flow Cytometric Analysis of ERBB Expression

Exponentially growing cells (1×10^6) were washed in ice-cold PBS and resuspended in 100 μmol/L PBS containing 0.1% (w/v) bovine serum albumin. Ten microliters of either rat anti-ERBB2 (clone ICR62-7.5 μg/mL) or rat anti-ERBB2

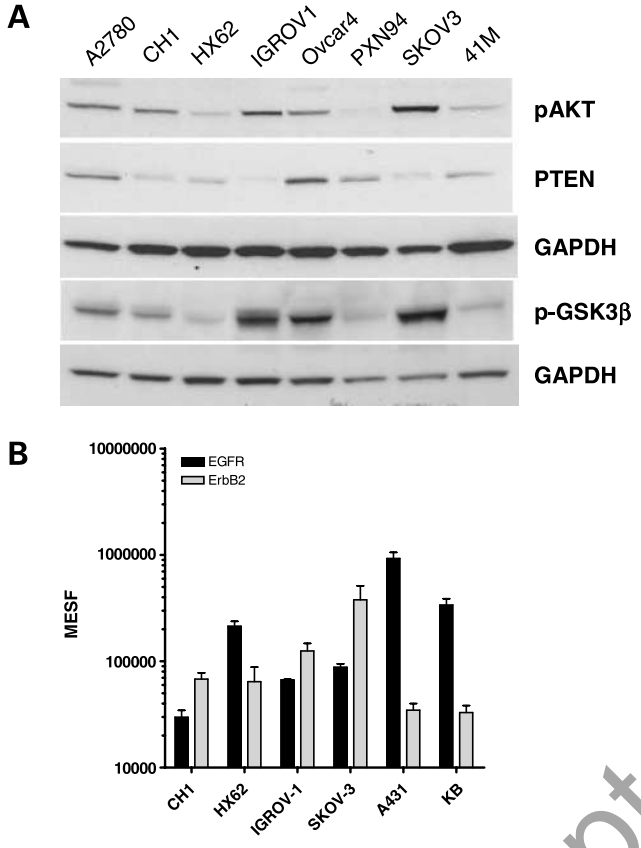

Figure 1. Expression levels of selected signaling proteins relevant to the activity of 17-AAG. **A**, a panel of eight human ovarian tumor cell lines was evaluated for the basal protein levels of p-AKT, p-GSK3β, and PTEN by Western blotting. GAPDH was used as a loading control. **B**, ErbB2 and EGFR levels were evaluated in some other lines. Surface expression of these proteins were measured by flow cytometry. Results are given as molecules of equivalent soluble fluorescein (*MESF*) using calibrated fluorescent beads.

(clone ICR55-7.5 μg/mL), both kind gifts from Dr. Sue Eccles (The Institute of Cancer Research), were added, and cells were incubated for 2 hours on ice. Following two washing steps in ice-cold PBS, cells were incubated with 100 μL FITC-conjugated anti-rat antibody (Sigma; 1:1,000) on ice and in the dark for 1 hour. Finally, cells were washed twice in ice-cold PBS before fixing in 0.1% (w/v) paraformaldehyde in PBS (Sigma) in preparation for flow cytometric analysis using the FACSCalibur (Becton and Dickinson, Oxford, United Kingdom). The most homogenous cell population was distinguished and gated by forward scatter and side scatter variables, and at least 5,000 events were recorded. The geometric-mean-FITC-fluorescence in each sample was measured and assessed using WinMDI v2.4.[3] This was converted to molecules of equivalent soluble fluorescein using calibrated fluorescent beads (DakoCytomation, Ltd., Copenhagen, Denmark).

Results

Characteristics of the Cell Line Panel

A panel of eight human ovarian tumor cell lines (A2780, CH1, HX62, IGROV-1, OVCAR-4, PXN94, SKOV-3, and 41M) was characterized for a number of key signaling proteins. From this panel, a minipanel of four lines (SKOV-3, IGROV-1, CH1, and HX62) was chosen for this present study based on the following properties. SKOV-3 and IGROV-1 cells express the highest level of p-AKT (phosphorylated at Ser^{473}) in the panel of eight lines (Fig. 1A). This activation was not sensitive to serum starvation and readdition and was therefore considered to be constitutive (data not shown) and in line with published data for SKOV-3 (24). The CH1 line was one of three lines (A2780, OVCAR-4, and CH1) to express a lower basal level of p-AKT that was nevertheless inducible by serum. The HX62 cell line was one of three lines (HX62, PXN94, and 41M) to have barely detectable levels of p-AKT (noninducible). These levels of p-AKT generally correlated well with the levels of the downstream effector, phospho-GSK3β (i.e., high basal levels in SKOV-3 and IGROV-1 cells compared with CH1 cells and barely detectable levels in HX62 cells; Fig. 1A). There are a number of points in growth factor downstream signaling that can contribute to constitutive AKT activation. For example, there is an increase in *PIK3CA* copy number in SKOV-3 cells (33). PTEN negatively regulates AKT through its phosphatase activity on PIP2/3, and whereas IGROV-1 cells are PTEN null (34), low expression has been reported in SKOV-3 (35). Our own data confirmed a virtually undetectable level of PTEN in these cell lines by Western blotting (Fig. 1A). However, levels were detectable in the other three cell lines but were lower than the positive control, OVCAR-4.[4] SKOV-3 cells also overexpress ERBB2 (36) and we compared its surface expression with the other cell lines in our minipanel (Fig. 1B). IGROV-1 cells were shown to express lower levels of ERBB2 consistent with other reports and CH1 and HX62 cells expressed even lower levels.[3] All lines expressed EGFR but at lower levels compared with the positive controls, KB and A431 epidermoid tumor cell lines (Fig. 1B). A431 cells express a moderate basal level of p-AKT (similar to CH1) that is inducible by serum, whereas KB cells express a very low level (noninducible; data not shown).

Activity of Paclitaxel and 17-AAG in Four Human Ovarian Tumor Cell Lines

Inhibition of cell growth was measured using an MTT assay as the end point. CH1 cells were shown to be sensitive to paclitaxel (IC_{50} = 6.6 nmol/L), whereas HX62, SKOV-3, and IGROV-1 cells were 6- to 10-fold less sensitive (Table 1). SKOV-3 cells were the most sensitive to 17-AAG and CH1 cells were the most resistant (IC_{50} ranged from 66 to 1,570 nmol/L). The wide range of sensitivity to 17-AAG relates, at least in part, to the level of DT-diaphorase/NQO1 expression (37). DT-diaphorase reduces

[3] http://facs.scripps.edu/software.html.

[4] http://dtp.nci.nih.gov/mtweb.

the benzoquinone moiety in 17-AAG to the more potent HSP90 inhibitor, 17-AAGH$_2$ (38). In the National Cancer Institute 60 cell line panel, the six ovarian cancer cell lines displayed activity of this bioreductive enzyme lower than the mean (0.65 μmol/min/mg protein) with values ranging from 0.053 to 0.45 μmol/min/mg protein.[3] The values for SKOV-3 and IGROV-1 were 0.11 and 0.13 μmol/min/mg protein, respectively. Another cell line comparison study reported that CH1 cells have enzyme activity <0.002 μmol/min/mg protein, consistent with the low sensitivity of these cells to 17-AAG (37).

17-AAG can lead to cell cycle arrest in either G_1 or G_2-M depending on the cell lines (17, 39, 40). We observed G_1 arrest in CH1 and IGROV-1 cells (both *p53* wild type; refs. 41, 42), and both a G_1 and G_2 arrest in the SKOV-3 (p53 null) and HX62 cells (*p53* mutant; ref. 40; data not shown). A similar association between expression of wild-type *p53*– and 17-AAG-induced G_1 arrest was observed in some colon tumor cell lines (39, 40). Paclitaxel induced a G_2-M arrest in all of the cell lines (data not shown). All the cell lines are RB positive as determined by detection of p-RB (Ser^{780}) protein by immunoblotting (data not shown).

Combination of 17-AAG with Paclitaxel or Carboplatin—Fixed Ratio Analysis

SKOV-3, IGROV-1, CH1, and HX62 ovarian tumor cells were simultaneously and continuously exposed to increasing equitoxic concentrations of paclitaxel and 17-AAG (~1:1 IC_{50} ratios) and growth inhibition was measured. CI values at $fu_{0.50}$ and the average CI values of $fu_{0.25,0.5,0.75}$ are given in Table 2. Values significantly less than 1 were obtained for SKOV-3 cells and IGROV-1 cells (mean CI at $fu_{0.5}$ = 0.53 and 0.50, respectively), demonstrating that the two drugs interact synergistically to inhibit growth (example plot given in Fig. 2A). In contrast, values significantly less than 1 were obtained for CH1 and HX62 cells, indicating antagonism (mean CI at $fu_{0.5}$ = 3.0 and 6.3, respectively). In the EGFR-overexpressing epidermoid KB and A431,17-AAG and paclitaxel were antagonistic and weakly synergistic, respectively (Table 2).

The order of addition of the two drugs was evaluated in CH1 cells in which antagonism had been observed when the drugs were added simultaneously. Cells were exposed to either paclitaxel or 17-AAG for 4 hours [IC_{50} = 65 ± 6.2 and 6,000 nmol/L (n = 2), respectively] followed by drug washout and the addition of the other drug for 92 hours. Sequencing 17-AAG first still gave antagonism, whereas paclitaxel first gave additivity (Table 2).

SKOV-3 and IGROV-1 cells were exposed simultaneously to 17-AAG and carboplatin at a fixed ratio of their IC_{50}. This combination was antagonistic in SKOV-3 cells (CI at $fu_{0.50}$ = 2.3 ± 1.4). An example CI plot is given in Fig. 2B. The data for IGROV-1 cells suggested additivity/slight antagonism (CI at $fu_{0.50}$ = 1.3 ± 0.21).

Combination of Paclitaxel and 17-AAG—Fixed Concentration (Sensitization) Experiments

SKOV-3 cells were exposed to a low, non–growth-inhibitory concentration of 17-AAG (6 nmol/L; 10% of IC_{50}) and increasing concentrations of paclitaxel. As might be expected, cell cycle phase distribution was not affected at this 17-AAG concentration (data not shown). The IC_{50} for paclitaxel decreased 3-fold under these conditions (i.e., from 70 to 23 nmol/L; mean of two independent experiments; Fig. 3A). The CI values at $fu_{0.5}$ were 0.47 in each of the two experiments. These data clearly show that a concentration of 17-AAG, essentially devoid of growth inhibitory effects, can nonetheless sensitize SKOV-3 cells to paclitaxel. In similar experiments done with IGROV-1 cells, the paclitaxel IC_{50} was reduced from 37 to 10 nmol/L (mean of two independent experiments) upon the addition of 100 nmol/L 17-AAG (a concentration that alone induces ~5% growth inhibition). This effect was ascribed to synergy because the CI at $fu_{0.5}$ were 0.63 and 0.51.

Effect of the Combination of Paclitaxel and 17-AAG on Induction of Cell Death

SKOV-3 cells were exposed to 80 nmol/L 17-AAG or 50 nmol/L paclitaxel (approximate respective IC_{50} values in the 96 hours MTT assay) or to the combination, and the attached and detached cells were counted at 24 hours. The individual agents did not significantly reduce the number of attached cells at this time but the combination led to an ~50% reduction compared with controls (data not shown). The detached cell number for the individual drugs was similar to control at 24 hours (i.e., ~8% of total cells), but ~45% of cells were detached in the presence of both drugs (Fig. 4A). Furthermore, the detached cells displayed apoptotic morphology (data not shown) and cleaved PARP was clearly visible by immunoblotting (Fig. 4B). These data are consistent with the synergy observed in the MTT assay being attributable to an earlier induction of apoptosis. Similar synergy at the level of apoptosis was confirmed in IGROV-1 and A431 cells (Fig. 4A). In contrast, the combination of IC_{50} concentrations of 17-AAG and paclitaxel in CH1 cells did not lead to a reduction in the attached cell number at 24 hours compared with the individual agents alone (data not shown). Although paclitaxel induced some detached apoptotic cells at 24 hours (~22% of total), the coaddition of 17-AAG did not lead to any further increase (Fig. 4A). Furthermore, the amount of cleaved PARP was not increased in the total CH1 cell population

Table 1. Inhibition of cell growth by paclitaxel and 17-AAG in four human ovarian and two epidermoid tumor cell lines

Cell line	Inhibition of cell growth, IC_{50} (nmol/L)	
	Paclitaxel	17-AAG
KB (epidermoid)	40 ± 9.1	16 ± 1.5
A431 (epidermoid)	36 ± 12	383 ± 46
SKOV-3 (ovarian)	65 ± 13	66 ± 7.8
IGROV-1 (ovarian)	43 ± 19	343 ± 21
HX62 (ovarian)	38 ± 9	686 ± 62
CH1 (ovarian)	6.3 ± 2.2	1,570 ± 310

NOTE: Cells were exposed to the agents continuously for 96 hours (CH1 and SKOV-3) or 72 hours (other lines) and growth inhibition was measured using the MTT assay as an end point. Results are given as mean ± SD ($n \geq 3$).

Table 2. CI values for the combination of 17-AAG and Taxol in cell lines

Cell line	Exposure conditions	CI at $fu_{0.5}$	Average CI at $fu_{0.25,0.50,0.75}$	Interpretation
KB (epidermoid)	72 h coexposure	2.1, 1.8	2.2 ± 0.63 (P = 0.076)	Antagonistic
A431 (epidermoid)	72 h coexposure	0.76 ± 0.095*	0.69 ± 0.15 (P = 0.072)	Weakly synergistic
SKOV-3 (ovarian)	96 h coexposure	0.53 ± 0.12†	0.51 ± 0.12*	Synergistic
IGROV-1 (ovarian)	72 h coexposure	0.50 ± 0.026†	0.45 ± 0.14*	Synergistic
HX62 (ovarian)	72 h coexposure	4.6 ± 2.0*	4.0 ± 0.87*	Antagonistic
CH1 (ovarian)	96 h coexposure	3.0 ± 1.0*	2.8 ± 0.47*	Antagonistic
CH1	Taxol (4 h) → 17-AAG (92 h)	0.96 ± 0.040	1.1 ± 0.33	Additive
CH1	17-AAG (4 h) → Taxol (92 h)	1.4, 1.9	1.8 ± 0.29*	Antagonistic

NOTE: CI values given at $fu_{0.50}$. The average CI is the average of the mean CI values at $fu_{0.25,0.50,0.75}$. CI <1, synergy; CI >1, antagonism; CI ~1.0, additivity.
*$P < 0.05$.
†$P < 0.005$ (one sample, two-tailed t test compared with 1.0).

treated with both agents compared with paclitaxel alone at 24 hours (Fig. 4B). Increasing the concentration of paclitaxel 3-fold (to 15 nmol/L) led to more detached apoptotic cells at 24 hours (~32%) but coaddition of 17-AAG reduced this to ~10% (Fig. 4A).

In experiments described earlier, 6 nmol/L 17-AAG (a non–growth-inhibitory concentration) sensitized SKOV-3 cells to paclitaxel using the MTT assay as an end point. As might be expected, 6 nmol/L 17-AAG alone did not lead to a reduction in attached cells compared with controls (up to 72 hours; Fig. 3B). However, when this concentration was combined with 50 nmol/L paclitaxel (~IC_{50}), the number of attached cells was reduced at all time points compared with paclitaxel alone. Furthermore, the number of detached cells was higher at 24 hours compared with paclitaxel alone (Fig. 3C), ~38% and ~8%, respectively. This was associated with an increase in cleaved PARP in the total cell population (Fig. 3D).

Effect of 17-AAG on Client Protein Depletion and Downstream Effectors

The exposure time and concentration dependence of 17-AAG-mediated depletion of selected HSP90 client proteins and their downstream effectors was examined in SKOV-3 cells. An increase in inducible HSP70 was used as a

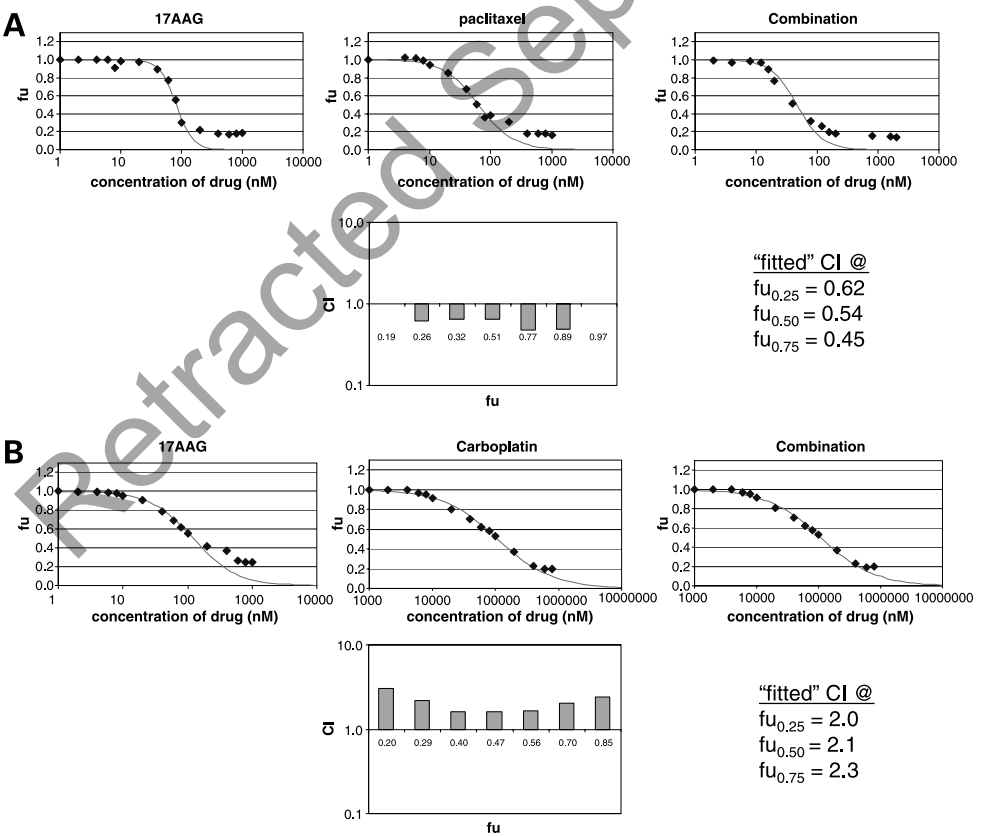

Figure 2. Examples of median-effect analysis in SKOV-3 cells in which 17-AAG was combined with paclitaxel (**A**) and carboplatin (**B**), demonstrating synergy and antagonism, respectively. Both drugs in the combination were added at a fixed ratio (of the IC_{50} of each individual drug) and the effects were analyzed using an in-house spreadsheet (part of which is shown in the figure) based on the median-effect analysis of Chou and Talalay (29). The concentrations of each agent alone, and the total concentration of both drugs together, are plotted against cell growth (as determined by an MTT assay) as fu values, with 1.0 being the uninhibited control value. The histogram gives the CI values for the fu values in the near linear part of the fu/concentration (~0.2–0.8 fu) using the mutually nonexclusive assumption. The best-fit CI values at $fu_{0.25}$, $fu_{0.5}$, and $fu_{0.75}$ are also included.

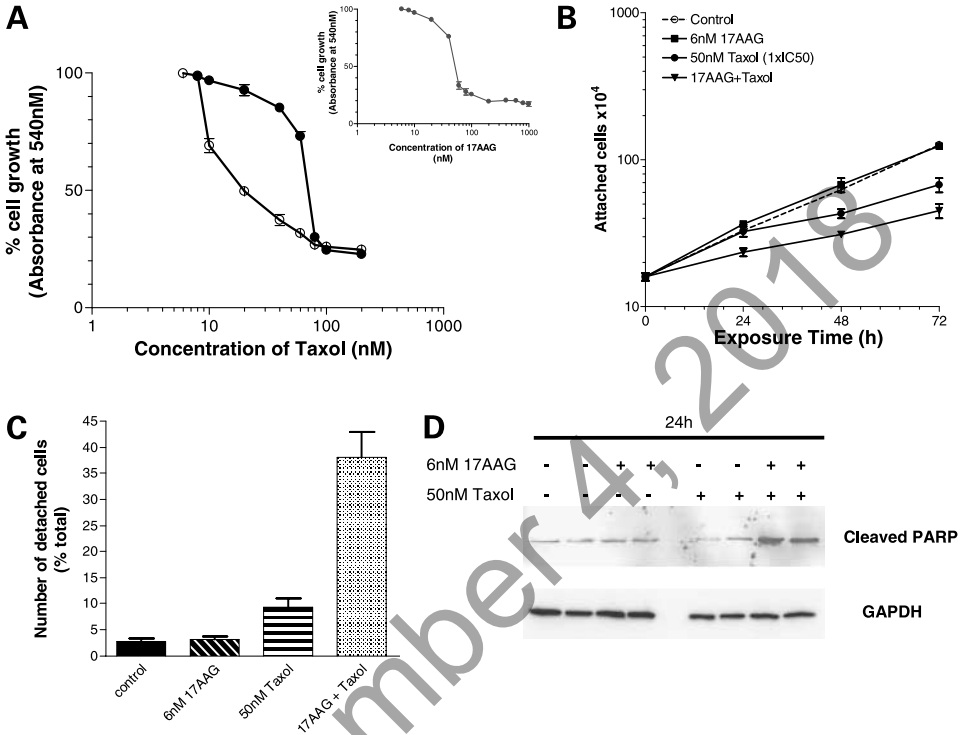

Figure 3. Effect of a non–growth-inhibitory concentration of 17-AAG on paclitaxel-induced growth inhibition in SKOV-3 cells. The growth inhibition curve (MTT assay) is given for paclitaxel (●; **A**) and for 17-AAG (*inset*). The effect of combining a non–growth-inhibitory concentration of 17-AAG (6 nmol/L) with paclitaxel is also shown (○; **A**). The results are given as the range of two independent experiments. The IC_{50} ($fu_{0.5}$) for paclitaxel decreased from 70 to 23 nmol/L in the presence of 6 nmol/L 17-AAG (CI at fu_{50} = 0.47). The attached cell number is displayed in **B** over 72 h for control (*dotted line*), 6 nmol/L 17-AAG (■), 50 nmol/L paclitaxel (●), and the combination of the two (▼). The detached cell number is expressed as a percentage of total cells (attached and detached) at 24 h (**C**). Results shown are the mean and range of two independent experiments. The nuclei of the detached cells were visually confirmed to be largely apoptotic using Geisma staining. Cleaved PARP was measured in the total cell population by immunoblotting (**D**) and the results for two independent experiments are given. GAPDH was used as a loading control.

sensitive marker of HSP90 inhibition (43, 44). Figure 5A shows the effect of 60 and 180 nmol/L 17-AAG (1 × IC_{50} and 3 × IC_{50}, respectively) at 4, 8, 16, and 24 hours. The proteins most sensitive to HSP90 inhibition that we examined were ERBB2 and HSP70, markedly decreasing and increasing, respectively, at 4 hours following exposure to 60 nmol/L 17-AAG. C-RAF and p-AKT were decreased at the 16-hour time point (8 hours after exposure to 180 nmol/L 17-AAG). Although HSP90 maintains the phosphorylation status of AKT, p-AKT can also be reduced as a result of 17-AAG-induced reduction in ERBB signaling. Total AKT was not markedly reduced unless cells were exposed to 200 nmol/L 17-AAG for 24 hours (data not shown). p-ERK 1/2 was decreased at 8 hours and very noticeably at 24 hours following exposure to 60 nmol/L 17-AAG (Fig. 5A). This marker of C-RAF signaling was markedly depleted 4 hours following exposure to 180 nmol/L 17-AAG (3 × IC_{50} concentration). Similar experiments were done on IGROV-1 cells exposed to equitoxic concentrations of 17-AAG. At the IC_{50} (300 nmol/L 17-AAG), ERBB2 was reduced at 16 hours and C-RAF and p-AKT at 24 hours (later than in SKOV-3). At 3 × IC_{50}, both markers were reduced at 16 hours (data not shown). CH1 cells were exposed to 1.8 and 5.4 μmol/L 17-AAG (~1 × IC_{50} and 3 × IC_{50}, respectively) for 4, 8, 16, and 24 hours (Fig. 5B). An increase in HSP70 was observed after 4-hour exposure to 1.8 μmol/L. C-RAF reduction became more marked with time, and p-ERK and p-AKT were markedly reduced at 8 and 16 hours, respectively. The effects on all these markers were earlier (or more marked) at the higher concentration of 17-AAG.

Results described earlier in this article showed that at a very low or non–growth-inhibitory concentration of 17-AAG could sensitize IGROV-1 and SKOV-3 cells to paclitaxel. We therefore examined the effect of these low concentrations of 17-AAG on HSP90 inhibition and client protein reduction. IGROV-1 cells were exposed to 100 nmol/L 17-AAG (1/3 IC_{50}; ~5% growth inhibition) and a reduction in ERBB2 was observed at 16 hours and a decrease in p-AKT (but not C-RAF) at 24 hours (data not shown). SKOV-3 cells exposed to 6 nmol/L 17-AAG (1/10 IC_{50}; non–growth inhibitory) for 4, 8, 16, and 24 hours had a markedly increased level of HSP70 at all time points, but C-RAF and p-ERK remained at control levels (Fig. 6A). However, there was a marked reduction in the level of ERBB2 at 16 hours and p-AKT at 24 hours (Fig. 6A). In contrast with effects in SKOV-3 cells, the effects of an equitoxic concentration of 17-AAG in CH1 cells (150 nmol/L 17-AAG; ~1/10 of the IC_{50}) were less marked with only a small increase in HSP70 observed at 24 hours and no apparent changes to c-RAF, p-ERK, or p-AKT (data not shown).

Effect of the Combination of 17-AAG and Paclitaxel on Client Proteins and Downstream Effectors

In SKOV-3 cells, 50 nmol/L paclitaxel (~IC_{50}) did not induce any apparent changes to the levels of HSP70, ERBB2, C-RAF, p-ERK, or p-AKT at 4, 8, 12, and 24 hours (Fig. 7; data not shown). Similar to the results described above, 80 nmol/L 17-AAG (~IC_{50}) led to a marked increase in HSP70 and decreased ERBB2 at 8 hours and at later time points. The level of these proteins in cells coexposed to 50 nmol/L paclitaxel and 80 nmol/L 17-AAG

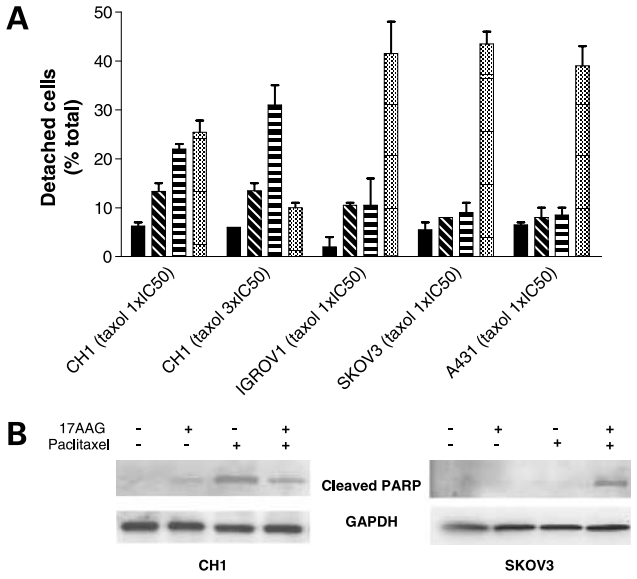

Figure 4. The effect of 17-AAG and paclitaxel individually and combined on induction of cell detachment and apoptosis. **A,** detached cell population as a percentage of total cells. Controls (*solid columns*) and after 24 h exposure to ~IC_{50} concentrations of 17-AAG (CH1, 1.5 μmol/L; IGROV-1, 0.36 μmol/L; SKOV-3, 0.08 μmol/L and A431, 0.34 μmol/L; *hatched columns*) and to ~IC_{50} concentrations of paclitaxel (CH1, 0.005 μmol/L; IGROV-1, 0.06 μmol/L; SKOV-3, 0.05 μmol/L and A431, 0.03 μmol/L; *horizontal columns*). *Cross-hatched columns,* effect of combining the two drugs. CH1 cells were also exposed to a higher concentration of paclitaxel (0.015 μmol/L; ~3 × IC_{50}) and the effect of addition of 1.5 μmol/L 17-AAG is displayed. **B,** cleaved PARP was measured by immunoblotting in extracts of SKOV-3 and CH1 cells exposed to ~IC_{50} concentrations of 17-AAG and paclitaxel either alone or in combination. GAPDH was used as a loading control.

were very similar to those for 17-AAG alone (Fig. 7). The 17-AAG-induced reduction in p-AKT at 12 and 24 hours was not affected by the coaddition of paclitaxel. Interestingly, the 17-AAG-induced reduction in C-RAF and p-ERK at these times was not observed in the combination (Fig. 7). Six-nanomolar 17-AAG is non–growth inhibitory; nevertheless, this paclitaxel-sensitizing concentration of 17-AAG is associated with increased HSP70 and decreased levels of ERBB2 and p-AKT but not of C-RAF or p-ERK. Similar changes in these proteins were observed when 50 nmol/L paclitaxel (IC_{50}) was added in addition to the 17-AAG (Fig. 6B).

The coaddition of 5 nmol/L paclitaxel (~IC_{50}) and 1,800 nmol/L 17-AAG (~IC_{50}) to CH1 cells did not affect the 17-AAG-induced increase in the level of HSP70 or reduction in p-AKT (Fig. 8). In contrast with the results with SKOV-3 cells, the combination did lead to a reduction in C-RAF and p-ERK that was similar to that seen with 17-AAG alone.

Discussion

Ovarian cancer is frequently sensitive to paclitaxel and carboplatin; however, following relapse, treatment options become more limited (45). Some patients remain chemosensitive and can be retreated with the same therapy until the disease becomes highly refractory to conventional treatment. Novel molecularly targeted agents may offer promise for the future in the treatment of ovarian cancer at any stage of the disease. Inhibitors of HSP90, such as 17-AAG, interfere with signaling pathways that are central to tumor growth and its metastatic spread (8–13). Preclinical studies have shown that 17-AAG may be combined effectively with conventional agents in a number of preclinical models (17, 39) and these include the agents particularly relevant to ovarian cancer. We have now shown the potential for 17-AAG to be combined with paclitaxel in ovarian cancer. However, we emphasize the need to better understand issues such as mechanism of action and molecular context so that ultimately the combination can be targeted at those patients most likely to respond.

The combination of 17-AAG and paclitaxel was synergistic in the two cell lines with a constitutively activated AKT (IGROV-1 and SKOV-3). The ability of 17-AAG to reduce p-AKT levels is therefore central to our studies, and a comparison was made between the molecular effects of 17-AAG on HSP90 inhibition in the SKOV-3 and CH1 ovarian tumor cells, in which the synergy was not seen. 17-AAG mediated reductions in C-RAF, p-ERK, and p-AKT in both cell lines. Changes were also observed in SKOV-3 cells but not CH1 cells at low, non–growth-inhibitory concentrations of 17-AAG. However, these effects at low concentrations were confined to reductions in ERBB2 and p-AKT and not to C-RAF or p-ERK. Similar results to SKOV-3 cells were obtained in IGROV-1 cells. The fact that these low concentrations were all that was required to sensitize SKOV-3 and IGROV-1 cells to paclitaxel further implicates inhibition of PI3K/AKT signaling as a crucial mediator of 17-AAG-induced sensitization to paclitaxel. These data also suggest that although full activity of this pathway is not critical for proliferation in SKOV-3 and IGROV-1 cells, it is essential in mediating paclitaxel resistance in these cells. Our results confirm the importance of inhibiting the PI3K/AKT pathway as one method for overcoming resistance in ovarian cancer. In contrast to the results with SKOV-3 and IGROV-1 cells, CH1 cells, which have a lower basal level of p-AKT, are more sensitive to paclitaxel and are not sensitized further by the addition of 17-AAG. This may suggest that p-AKT is not a critical mediator of paclitaxel resistance in CH1 cells. In partial support of this hypothesis is the fact that although stable transfection of CH1 cells with ERBB2 (CH1:ERBB2) increased the level of p-AKT and sensitized them to 17-AAG (10-fold), the combination with paclitaxel remained antagonistic.[5] However, there could be an alternative explanation for the different effects of the paclitaxel/17-AAG combination between cell lines based on the effect paclitaxel may have on 17-AAG-induced effect on cell signaling. Paclitaxel prevented the 17-AAG-induced reduction in C-RAF signaling in SKOV-3 cells when both

[5] Unpublished data.

agents were combined at their respective IC_{50} concentrations. Similar results to SKOV-3 were obtained using A431 epidermoid cells in which the combination was synergistic (data not shown). In contrast, paclitaxel did not affect 17-AAG-mediated inhibition of C-RAF signaling in CH1 cells. Although the reasons are unclear, it is therefore possible that 17-AAG-mediated inhibition of ERK signaling in CH1 cells opposes the drug sensitization effects of reduced AKT signaling to an extent not seen in SKOV-3 cells.

The role that ERBB family member overexpression plays in mediating synergy when 17-AAG and paclitaxel are combined is unclear. ERBB2 is regarded as one of the most sensitive client proteins to HSP90 inhibition (13). Munster et al. (46) showed that although 17-AAG led to degradation of ERBB2 in a number of ERBB2-expressing cell lines, only in tumors in which it was overexpressed did depletion of ERBB2 seem to be linked to growth arrest and apoptosis. However, the situation may be different when 17-AAG is used to sensitize to cytotoxic drugs by inhibiting survival pathways. SKOV-3 cells overexpress ERBB2, and when these cells are exposed to 17-AAG, a rapid reduction in ERBB2 was observed followed by a reduction in p-AKT. However, IGROV-1 cells express EGFR and ERBB2 at average levels and exposure to low concentrations of 17-AAG also led to a rapid reduction in the level of ERBB2 and sensitization to paclitaxel. Interpretation of these data is complicated by the fact that the phosphorylation status of AKT is maintained by HSP90, making it difficult to conclude whether the observed effect on p-AKT is directly related to 17-AAG-mediated destabilization of p-AKT rather than as an indirect result of ERBB2 reduction. Both mechanisms could apply and further work is needed to deconvolute the importance of each. The effect of other ERBB family members, such as EGFR, on the outcome of this combination is unclear. The HX62 line expresses high levels of EGFR but has low levels of p-AKT (noninducible by serum) and antagonism was observed with 17-AAG and paclitaxel. The A431 and KB epidermoid cell lines

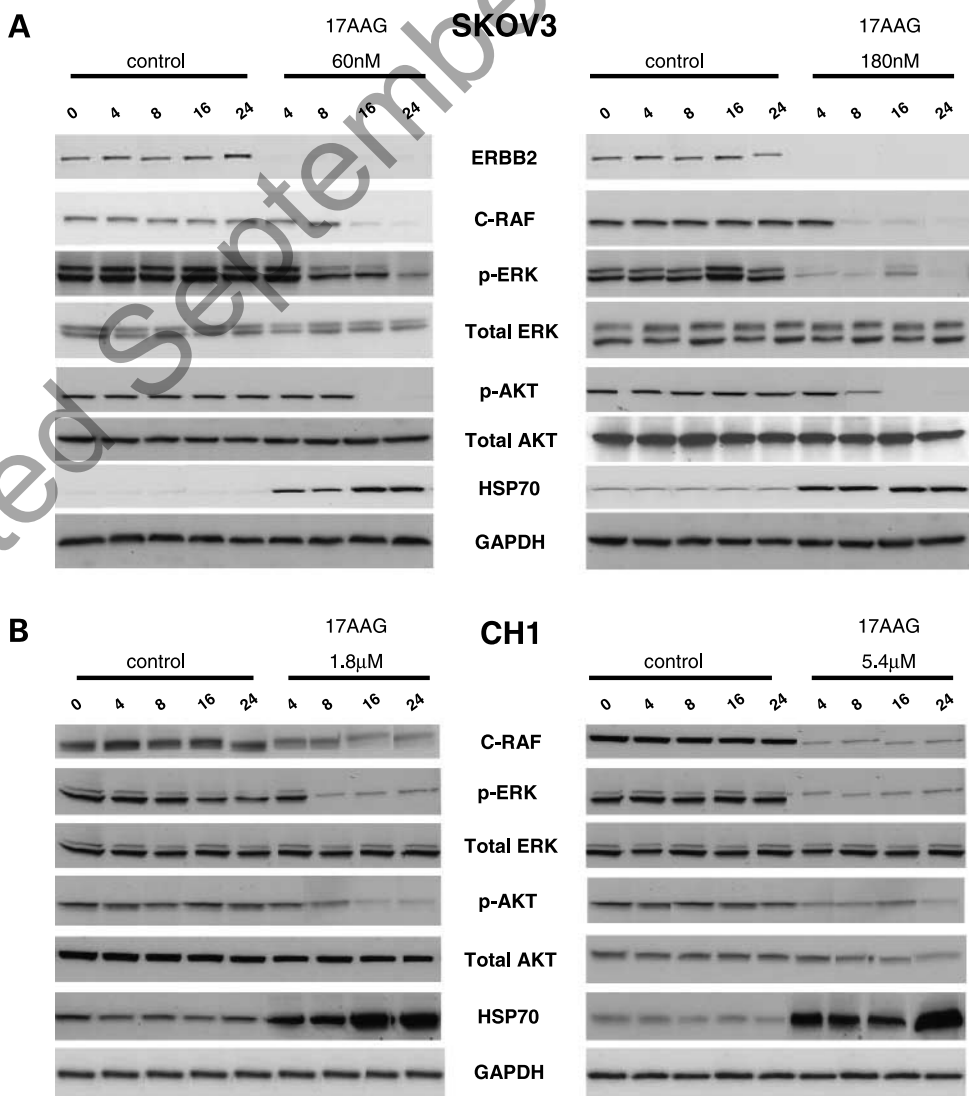

Figure 5. Effect of 17-AAG on markers of HSP90 inhibition in SKOV-3 and CH1 ovarian tumor cells. SKOV-3 (**A**) and CH1 (**B**) cells were exposed to $\sim 1 \times IC_{50}$ and $3 \times IC_{50}$ concentrations of 17-AAG and were harvested at the times indicated (4–24 h), extracts were made, and proteins were measured by immunoblotting as described in Materials and Methods. GAPDH was used as a loading control. Representative blots of a least two independent experiments.

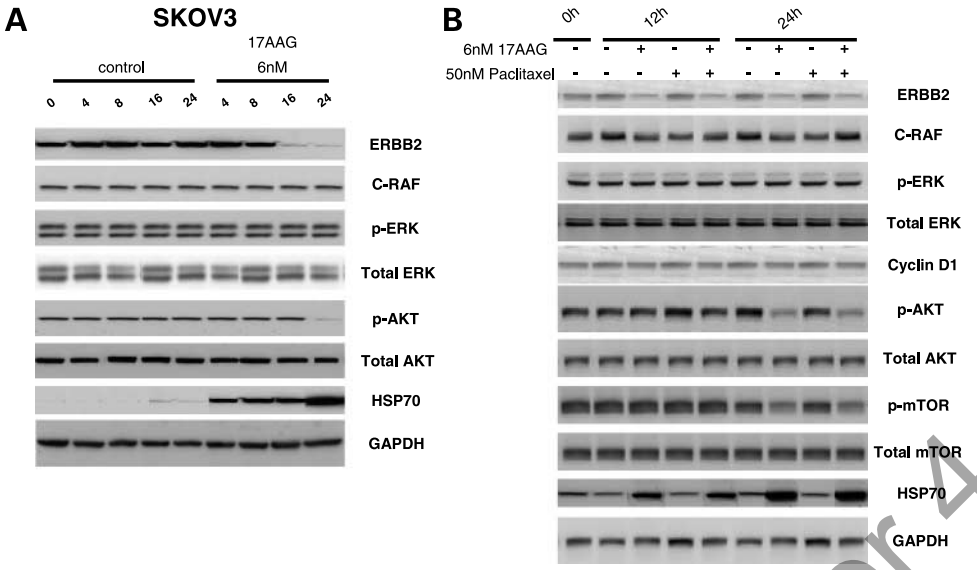

Figure 6. Effect of a non–growth-inhibitory concentration of 17-AAG alone and in combination with paclitaxel on markers of HSP90 inhibition in SKOV-3 cells. SKOV-3 cells were exposed to 6 nmol/L 17-AAG (**A**) and harvested at the times indicated (4–24 h), extracts were made, and proteins were measured by immunoblotting. GAPDH was used as a loading control. The experiment was repeated in the presence and absence of 50 nmol/L paclitaxel (an IC_{50} concentration; **B**).

overexpress EGFR; however, whereas A431 cells express a moderate basal level of p-AKT, KB cells express a very low basal level of p-AKT (not inducible). The combination of 17-AAG and paclitaxel was weakly synergistic and antagonistic in A431 and KB, respectively.

Taking all the cell line data together, we can summarize the results as follows: synergy was observed in SKOV-3 (overexpressed ERBB2, high p-AKT) and IGROV-1 (high p-AKT); weak synergism was seen in A431 (overexpressed EGFR, moderate p-AKT); and antagonism was observed in CH1 (moderate p-AKT), HX62 (overexpressed EGFR, low p-AKT), and KB cells (overexpressed EGFR, low p-AKT). A reasonable hypothesis that needs to be tested further is that 17-AAG and paclitaxel are synergistic in cell lines that have an activated AKT pathway mediating paclitaxel resistance, driven at least in part by ERBB (over)expression. However, the fact that CH1:ERBB2 cells (discussed earlier) were not sensitized to paclitaxel by 17-AAG illustrates the complexity of the mechanisms involved and/or the limitations of these types of model. Currently, we are attempting to stably knock down AKT1/2 in SKOV-3 cells with short hairpin RNA to provide an alternative experimental model. It is important to address the question of pharmacologic relevance of our results, particularly as we have evaluated the combination in cell lines with very different intrinsic sensitivities to 17-AAG. SKOV-3 cells are relatively sensitive in that the IC_{50} (66 nmol/L) is lower than the mean IC_{50} in a panel of 26 human ovarian and colon tumor cell lines (220 nmol/L; ref. 37) or the National Cancer Institute 60 cell line panel (120 nmol/L).[3] Furthermore, we found that as little as 6 nmol/L 17-AAG sensitized SKOV-3 cells to paclitaxel. On the other hand, CH1 cells are relatively resistant to 17-AAG (IC_{50} = 1,600 nmol/L), which relates to very low DT-diaphorase activity (37). Median-effect analysis is usually done at a fixed ratio of the IC_{50} of the two drugs and therefore the question arises as to the

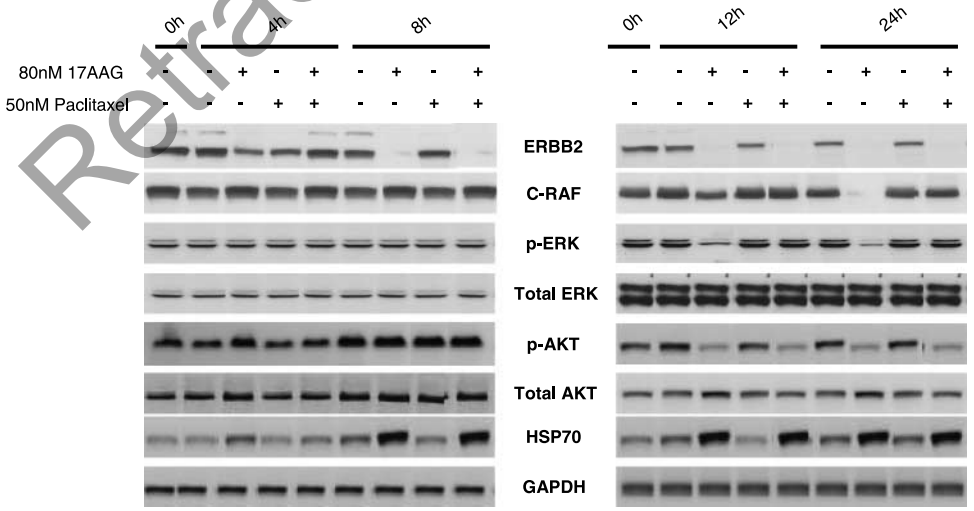

Figure 7. Effect of 17-AAG and paclitaxel alone and in combination on markers of HSP90 inhibition in SKOV-3 cells. SKOV-3 cells were exposed to 80 nmol/L 17-AAG and 50 nmol/L paclitaxel (~IC_{50} concentrations) and the combination of both drugs for 4 to 24 h. Proteins were measured in cell extracts by immunoblotting with GAPDH as a loading control.

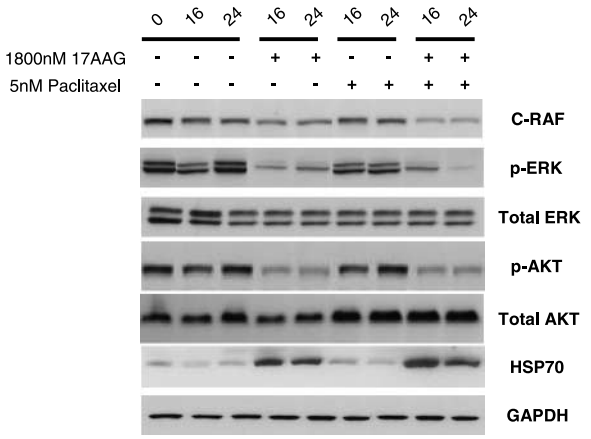

Figure 8. Effect of 17-AAG and 5 nmol/L paclitaxel alone and in combination on markers of HSP90 inhibition in CH1 cells. CH1 cells were exposed to 1,800 nmol/L 17-AAG and 5 nmol/L paclitaxel (IC_{50} concentrations) and the combination of both drugs for 16 to 24 h. Proteins were measured in cell extracts by immunoblotting with GAPDH as a loading control.

clinical significance of the concentrations used. The plasma levels at the recommended phase II dose on a weekly schedule of 450 mg/m^2/wk are ~120 nmol/L for at least 24 hours (14). Thus, the concentrations that sensitized SKOV-3 and IGROV-1 cells (~10–100 nmol/L) are easily achievable. In contrast, the concentration of 17-AAG used in CH1 cells either alone or in combination was much higher and probably not achievable clinically. Novel inhibitors of HSP90 are being developed that are not metabolized by DT-diaphorase (10, 47). It will be important to evaluate such compounds in the human ovarian tumor cell line and xenograft models.

The combination of 17-AAG and carboplatin was antagonistic in SKOV-3 and additive/weakly antagonistic in IGROV-1 cells. Because these results contrast with those of paclitaxel, it can be proposed that the mechanism of action of the cytotoxic agent may be crucial in determining whether it can be combined successfully with 17-AAG. It has been suggested that 17-AAG-mediated inhibition of c-Jun-NH_2-kinase signaling can lead to antagonism when cisplatin and 17-AAG are combined (39). It will be necessary to further explore the effect of order of addition of these drugs and effects on other human ovarian tumor cell lines.

In summary, this study suggests that 17-AAG has the potential to be synergistic with paclitaxel in some human ovarian tumors. Importantly, we have shown that 17-AAG does not necessarily have to be given at a concentration that alone affects proliferation or induces apoptosis. This may, however, be restricted to a subset of tumors that are highly sensitive to 17-AAG-mediated reduction of ERBB2 and/or p-AKT levels. Further work will expand this study to other models of ovarian cancer, including additional isogenic lines engineered for stable knockdown or expression of proteins such as AKT and ERBB2, and to newer inhibitors of HSP90 so that we can inform subsequent clinical studies with HSP90 inhibitors in humans. Retreatment with paclitaxel and/or carboplatin comprises an important element of current therapy for relapsed ovarian cancer. Our data support the view that the efficacy of retreatment with paclitaxel, but not necessarily carboplatin, may be increased by coadministration of 17-AAG (or potentially other inhibitors of PI3K/AKT signaling). However, this benefit may be limited to patients whose tumors have a defined molecular signature. Our studies should ultimately help guide clinical investigators to select patients who are likely to benefit from this type of combined therapy.

References

1. Workman P, Kaye SB. Translating basic cancer research into new cancer therapeutics. Trends Mol Med 2002;8:S1–9.
2. Druker BJ. STI571 (Gleevec™) as a paradigm for cancer therapy. Trends Mol Med 2002;8:S14–8.
3. Hanahan D, Weinberg RA. The hallmarks of cancer. Cell 2000;100:57–70.
4. Hynes NE, Lane HA. ErbB receptors and cancer: the complexity of targeted inhibitors. Nat Rev Cancer 2005;5:341–54.
5. Moroni M, Veronese S, Benvenuti S, et al. Gene copy number for epidermal growth factor receptor (EGFR) and clinical response to anti-EGFR treatment in colorectal cancer: a cohort study. Lancet Oncol 2005;6:257–8.
6. Sellers WR, Meyerson M. EGFR gene mutations: a call for global × global views of cancer. J Natl Cancer Inst 2005;97:326–8.
7. Jackman AL, Kaye S, Workman P. The combination of cytotoxic and molecularly targeted therapies—can it be done? Drug Discov Today 2004;1:445–54.
8. Workman P. Combinatorial attack on multistep oncogenesis by inhibiting the Hsp90 molecular chaperone. Cancer Lett 2004;206:149–57.
9. Sausville EA, Tomaszewski JE, Ivy P. Clinical development of 17-allylamino, 17-demethoxygeldanamycin. Cur Cancer Drug Targets 2003;3:377–83.
10. Dymock BW, Drysdale MJ, McDonald E, Workman P. Inhibitors of HSP90 and other chaperones for the treatment of cancer. Expert Opin Ther Patents 2004;14:837–47.
11. Neckers L, Neckers K. Heat-shock protein 90 inhibitors as novel cancer chemotherapeutic agents, an update. Expert Opin Emerg Drugs 2002;10:137–49.
12. Maloney A, Workman P. Hsp90 as a new therapeutic target for cancer therapy: the story unfolds. Exp Opin Biol Ther 2002;2:2–24.
13. Solit DB, Scher HI, Rosen N. Hsp90 as a therapeutic target in prostate cancer. Semin Oncol 2003;30:709–16.
14. Banerji U, O'Donnell A, Scurr M, et al. Phase I pharmacokinetic and pharmacodynamic study of 17-allylamino, 17-demethoxygeldanamycin on patients with advanced malignancies. J Clin Oncol 2005;23:4152–61.
15. Grem JL, Morrison G, Guo X-D, et al. Phase I and pharmacologic study of 17-(allylamino)-17-demthoxygeldanamycin in adult patients with solid tumours. J Clin Oncol 2005;23:1885–93.
16. Hu L, Hofman J, Lu Y, Mills GB, Jaffe RB. Inhibition of phosphatidylinositol 3-kinase increases efficacy of paclitaxel *in vitro* and *in vivo* ovarian cancer models. Cancer Res 2002;62:1087–92.
17. Munster PN, Bass A, Solit D, Norton L, Rosen N. Modulation of Hsp90 function by ansamycins sensitises breast cancer cells to chemotherapy-induced apoptosis in an RB and schedule-dependent manner. Clin Cancer Res 2001;7:2228–36.
18. Blagosklonny MV, Fojo T, Bhalla KN, et al. The Hsp90 inhibitor geldanamycin selectively sensitises Bcr-Abl-expressing leukaemia cells to cytotoxic chemotherapy. Leukemia 2001;15:1537–43.
19. Nguyen DM, Chen A, Mixon A, Schrump DS. Sequence-dependent enhancement of paclitaxel toxicity in non-small cell lung cancer by 17-allylamino 17-demethoxygeldanaycin. J Thorac Cardiovasc Surg 1999;118:908–15.
20. Solit DB, Basso AD, Olshen AB, Scher HI, Rosen N. Inhibition of heat shock protein 90 function down-regulates Akt kinase and sensitises tumours to Taxol. Cancer Res 2003;63:2139–44.

21. Basso AD, Solit DB, Munster PN, Rosen N. Ansamycin antibiotics inhibit Akt activation and cyclin D expression in breast cancer cells that overexpress HER2. Oncogene 2002;21:1159 – 66.

22. Vivanco I, Sawyers CL. The phosphatidylinositol 3-kinase-AKT pathway in human cancer. Nat Rev 2002;2:489 – 99.

23. Thompson JE, Thompson CB. Putting the Rap on Akt. J Clin Oncol 2004;22:4217 – 26.

24. Altomare DA, Wang HQ, Skele KL, et al. AKT and mTOR phosphorylation is frequently detected in ovarian cancer and can be targeted to disrupt ovarian tumour cell growth. Oncogene 2004;23:5853 – 7.

25. Mills GB, Lu Y, Fang X, et al. The role of genetic abnormalities of PTEN and the phosphatidylinositol 3-kinase pathway in breast and ovarian tumorigenesis, prognosis, and therapy. Semin Oncol 2001;28:125 – 41.

26. Yuan ZQ, Sun M, Feldman RI, et al. Frequent activation of AKT2 and induction of apoptosis by inhibition of phosphoinositide-3-OH kinase/Akt pathway in human ovarian cancer. Oncogene 2000;19:2324 – 30.

27. Page C, Lin HJ, Jin Y, et al. Overexpression of Akt/AKT can modulate chemotherapy-induced apoptosis. Anticancer Res 2000;20:407 – 16.

28. Hu L, Zaloudek C, Mills GB, Gray J, Jaffe RB. *In vivo* and *in vitro* ovarian carcinoma growth inhibition by a phosphatidylinositol 3-kinase inhibitor (LY294002). Clin Cancer Res 2000;6:880 – 6.

29. Hills CA, Kelland LR, Abel G, Siracky J, Wilson AP, Harrap KR. Biological properties of ten human ovarian carcinoma cell lines: calibration *in vitro* against four platinum complexes. Br J Cancer 1989;59:527 – 34.

30. Holford J, Sharp SY, Murrer BA, Abrams M, Kelland LR. *In vitro* circumvention of cisplatin resistance by the novel sterically hindered platinum complex AMD473. Br J Cancer 1998;77:366 – 73.

31. Twentyman PR, Luscombe M. A study of some variables in a tetrazolium dye (MTT) based assay for cell growth and chemosensitivity. Br J Cancer 1987;56:279 – 85.

32. Chou TC, Talalay P. Quantitative analysis of dose-effect relationships: the combined effects of multiple drugs or enzyme inhibitors. Adv Enzyme Regul 1984;22:27 – 55.

33. Shayesteh L, Lu Y, Kuo AL, et al. PIK3CA is implicated as an oncogene in ovarian cancer. Nat Genet 1999;21:99 – 102.

34. Cruet-Hennequart S, Maubant S, Luis J, Gauduchon P, Staedel C, Dedhar S. α_v integrins regulate cell proliferation through integrin-linked kinase (ILK) in ovarian cancer cells. Oncogene 2003;22:1688 – 702.

35. Arboleda MJ, Lyons JF, Kabbinavar FF, et al. Overexpression of AKT/protein kinase Bβ leads to upregulation of β1 integrins, increased invasion, and metastasis in human breast and ovarian cancer cells. Cancer Res 2003;63:196 – 206.

36. Xu F, Yu Y, Le X-F, Boyer C, Mills GB, Bast RC. The outcome of heregulin-induced activation of ovarian cancer cells depends on the relative levels of HER-2 and HER-3 expression. Clin Cancer Res 1999;5:3653 – 60.

37. Kelland LR, Sharp SY, Rogers PM, Myers TG, Workman P. DT-diaphorase expression and tumor cell sensitivity to 17-allylamino,17-demethoxygeldanamycin, an inhibitor of heat shock protein 90. J Natl Cancer Inst 1999;91:1940 – 9.

38. Guo W, Reigan P, Siegel D, Zirrolli J, Gustafson D, Ross D. Formation of 17-allylamino-demethoxygeldanamycin (17-AAG) hydroquinone by NAD(P)H:quinone oxidoreductase 1: role of 17-AAG hydroquinone in heat shock protein 90 inhibition. Cancer Res 2005;65:10006 – 15.

39. Vasilevskaya IA, Rakitina TV, O'Dwyer PJ. Quantitative effects on c-Jun N-terminal protein kinase signalling determine synergistic interaction of cisplatin and 17-allylamino-17-demethoxygeldanamycin in colon cancer cell lines. Mol Pharmacol 2004;65:235 – 43.

40. Hostein I, Robertson D, DiStefano F, Workman P, Clarke PA. Inhibition of signal transduction by the Hsp90 inhibitor 17-allylamino-17-demethoxygeldanamycin results in cytostasis and apoptosis. Cancer Res 2001;61:4003 – 9.

41. Walton MI, Koshy P, Medlow CJ, Sharp S, Kelland LR, Titley J. The role of functional P53 status in cisplatin chemosensitivity in a panel of human ovarian cancer cell lines. Br J Cancer 1998;78:19.

42. Zuco V, Zanchi C, Cassinelli G, et al. Induction of apoptosis and stress response in ovarian carcinoma cell lines treated with ST1926, an atypical retinoid. Cell Death Differ 2004;11:280 – 9.

43. Clarke PA, Hostein I, Banerji U, et al. Gene expression profiling of human colon cancer cells following inhibition of signal transduction by 17-allyamino-17-demethoxygeldanamycin, an inhibitor of the hsp90 molecular chaperone. Oncogene 2000;19:4125 – 33.

44. Whitesell L, Bagatell R, Falsey R. The stress response: implications for the clinical development of Hsp90 inhibitors. Cur Cancer Drug Targets 2003;3:349 – 58.

45. Agarwal R, Kaye SB. Ovarian cancer: strategies for overcoming resistance to chemotherapy. Nat Rev Cancer 2003;7:502 – 16.

46. Munster PN, Marchion DC, Basso AD, Rosen N. Degradation of HER2 by ansamycins induces growth arrest and apoptosis in cells with HER2 overexpression via a HER3, phophatidylinositol 3-kinase-AKT-dependent pathway. Cancer Res 2002;62:3132 – 7.

47. Cheung K-MJ, Matthews TP, James K, et al. The identification, synthesis, protein crystal structure and *in vitro* biochemical evaluation of a new 3,4-diarylpyrazole class of Hsp90 inhibitors. Bioorg Med Chem Lett 2005;15:3338 – 43.

Molecular Cancer Therapeutics

Retraction: Potentiation of Paclitaxel Activity by the HSP90 Inhibitor 17-allylamino-17-demethoxygeldanamycin in Human Ovarian Carcinoma Cell Lines with High Levels of Activated AKT

This article (1) is being retracted at the request of the authors. The work is in two main parts. The first part is a description of the relevant characteristics of the human ovarian cancer cell lines used and an analysis of the efficacy of the combination of the HSP90 inhibitor 17-AAG with paclitaxel and carboplatin. The latter part shows the effect of the single agents and drug combinations on HSP90 client proteins and downstream effectors. All of the experiments in the article were carried out in the laboratory of the senior author A.L. Jackman. It has been brought to our attention that in the second part of the article, Figs. 5A, 5B, 6, 7, and 8 contained inappropriately assembled Western blots. N. Sain performed the experiments and processed the data and has taken primary responsibility for the flawed figures. The authors wish to sincerely apologize to the scientific community and deeply regret any inconveniences or challenges resulting from the publication and subsequent retraction of this article.

Reference

1. Sain N, Krishnan B, Ormerod MG, De Rienzo A, Liu WM, Kaye SB, et al. Potentiation of paclitaxel activity by the HSP90 inhibitor 17-allylamino-17-demethoxygeldanamycin in human ovarian carcinoma cell lines with high levels of activated AKT. Mol Cancer Ther 2006;5:1197–208.

Published online September 4, 2018.
doi: 10.1158/1535-7163.MCT-18-0595

Molecular Cancer Therapeutics

Potentiation of paclitaxel activity by the HSP90 inhibitor 17-allylamino-17-demethoxygeldanamycin in human ovarian carcinoma cell lines with high levels of activated AKT

Nivedita Sain, Bhavani Krishnan, Michael G. Ormerod, et al.

Mol Cancer Ther 2006;5:1197-1208.